



# Probabilistic Corrosion-free Service Life of the RCC Structures Made with OPC and Ultra-fine Slag-based Binders

S. Athibaranan<sup>1\*</sup>, P. Chandru<sup>2</sup>, K. Nandhini<sup>3</sup> and A. Dhanalaksmi<sup>4</sup>

Department of Civil Engineering, GMR Institute of technology, Srikakulam, AP, India

Department of Civil Engineering, National Institute of technology Calicut, KL, India

Department of Civil Engineering, College of Engineering, Guindy, Chennai, TN, India

Department of Civil Engineering, PSR Engineering College, Sivakasi, TN, India

Received: 06.05.2024 Accepted: 17.07.2024 Published: 30.06.2024

\*athibaranan.s@gmrit.edu.in

## ABSTRACT

The primary factor in the deterioration of reinforced concrete is chloride-induced corrosion. It has a direct impact on the service life of the structure and has been the subject of much research over the past 5 decades. One of the most cost-effective ways to lessen chloride-induced corrosion was identified to be the use of more supplementary cementitious material (SCM). Moreover, when SCMs are ground down to a smaller size, the resulting particles serve as microfillers, which have a significant impact on the improvement of mechanical properties and durability. This paper highlights the influence of grinding slag into an Ultra Fine Slag (UFS) on chloride ion penetration in the mortar specimen. A bulk diffusion test was performed on a mortar replaced with UFS which show a synergic reduction in chloride diffusivity in comparison with control mixes. In addition, an attempt is made on prediction of probabilistic service life estimation by Error function model.

**Keywords:** Ultra fine slag; Service life prediction; Supplementary cementitious material; Chloride ion penetration.

## 1. INTRODUCTION

The service life is a main factor in the sustainability of reinforced structures especially, its cost. The repair and rehabilitation costs are more in order to prolong the service life of reinforced concrete structures (Jumaat *et al.* 2011). The detrimental effect such as, concrete cover cracking, decreased bonding between the concrete and steel rebar, reduced reinforcement dimensions, reduced ductility and yield strength of the steel rebar in reinforced concrete structures are due to corrosion of rebar by chloride ingress phenomenon (Andrade *et al.* 2011).

In most of the research, the simple and economical way to address this diffusion problem is by adding supplementary cementitious materials (Vivek *et al.* 2020). Even though a lot of research has been conducted, still lot of efforts are required to find a sustainable material for chloride induced corrosion (Angst *et al.* 2009). In this research, the response of ultra fine slag (UFS) against corrosion induced by chloride ingress is analyzed. In order to analyze the corrosion, it is required to find the apparent chloride diffusion, age coefficient and chloride threshold of the medium (Hooton *et al.* 1995). However, accurately predicting the service life of UFS concrete remains a complex challenge due to the inherent variability in material properties and

environmental conditions. Traditional deterministic models often fall short in capturing this variability, leading to conservative estimates or premature failures. To address this limitation, probabilistic approaches have gained traction, offering a more comprehensive understanding of the uncertainties involved. In this context, the application of probabilistic service life modeling utilizing the error function model presents a compelling avenue for advancing the reliability and accuracy of predictions for UFS concrete. The error function model, rooted in probabilistic theory, offers a versatile framework for characterizing the stochastic nature of deterioration processes, encompassing factors such as material properties, environmental exposure, and loading conditions.

By integrating probabilistic techniques with the error function model, researchers can effectively account for the inherent randomness and variability in UFS concrete performance, thereby yielding more realistic and robust predictions of service life. This approach not only enhances our ability to assess the long-term durability of UFS concrete but also facilitates informed decision-making in design, maintenance, and rehabilitation strategies. In this paper, we delve into the rationale behind adopting probabilistic methodologies for UFS concrete service life modeling, highlighting the significance of the error function model as a powerful

tool in this endeavor. Furthermore, we explore the challenges and opportunities associated with probabilistic modeling in the context of UFS concrete, underscoring its potential to revolutionize the way we approach durability assessment and sustainability in infrastructure construction. Comprehensive analysis coupled with insights from ongoing research endeavors a deeper exploration of probabilistic service life modeling of UFS concrete using the error function model.

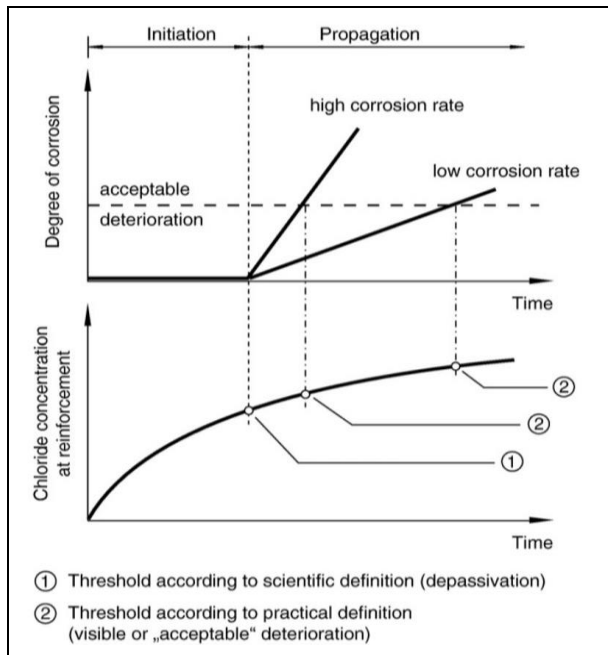


Fig. 1: Corrosion model (Andrade et al. 2011)

The 2-definition given in Fig. 1 explains the initiation and propagation of the corrosion in rebars by action of chloride ingress (Andrade et al. 2017). The UFS is a granulated slag with value added material ground in a ball mill attached with high efficiency classifier, which classifies the material and ensures that only the required micro size particle enters the final product (Petcherdchoo et al. 2013).

## 2. MATERIALS AND METHODS

### 2.1 Material Properties

The Ordinary Portland Cement (OPC) of 43 grade is used which is having a specific gravity of 3.16 and specific surface area of 342 m<sup>2</sup>/kg (Table 1). The UFS is particles of ground granulated blast-furnace slag with size lower than 10 micrometre. The UFS has a specific gravity of 2.93 and specific surface area of 2435 m<sup>2</sup>/kg.

### 2.2 Mix Characterization

The binary blend is made by replacing OPC with UFS at 5%, 10%, 15%, 20% and 25%. A water binder

ratio of 0.4 is fixed after going through consistency test. The cylindrical specimen of size 100mm diameter and 50 mm height is casted and demoulded in 24 hours and kept for 28 days water curing for the determination of apparent chloride diffusion coefficient and chloride threshold concentration. The material is weighed using weight balance and a digital mortar mixture is used to blend cementitious material and sand. The fresh mix is put inside the moulds of size 100 mm diameter and 50 mm height and 50 mm diameter and 100 mm height, respectively and compacted using vibrating table and is demoulded after 1 hour and kept for water curing. The proportions are made based on ASTM C109 and are shown in the Table 2.

Table 1. The composition and properties of materials

Composition and properties of materials		
Oxides	OPC	UFS
SiO <sub>2</sub>	19.9	35.2
Al <sub>2</sub> O <sub>3</sub>	4.62	12.6
Fe <sub>2</sub> O <sub>3</sub>	3.97	0.4
MgO	1.73	5.5
CaO	64.27	42.4
Na <sub>2</sub> O		0.3
K <sub>2</sub> O	0.57	0.44
Total Sulphur as SO <sub>3</sub>	2.56	0.2
Fineness (m <sup>2</sup> /kg) (Blaine's air permeability)	342	2435
Specific gravity	3.14	2.92

Table 2. Mix proportion of mortar with and without UFS

Binder Content	OPC	UFS	Fine aggregate	W/B
OPC	1	0	2.75	0.4
UFS05	0.95	0.05	2.75	0.4
UFS10	0.90	0.10	2.75	0.4
UFS15	0.85	0.15	2.75	0.4
UFS20	0.80	0.20	2.75	0.4
UFS25	0.75	0.25	2.75	0.4

### 2.3 Experimental Studies

A Nord test NT Build 443 bulk diffusion test was conducted on cylindrical specimens with a diameter of 100 mm and a height of 50 mm, that were water cured for 28 days, in order to estimate the diffusion co-efficient (Dcl) for the various concrete mixes. In accordance with ASTM C1556 (Jumaat et al. 2011), cylindrical specimens coated with epoxy around their circumference alone were submerged in 2.8M NaCl solution for 56 days following their initial immersion in saturated Ca(OH)<sub>2</sub> solution. Concrete powder samples were ground to a depth of 25 mm below the concrete surface in order to generate chloride profiles (i.e., at 0-1, 1-2, 2-3, 3-4, 4-6, 8-10, 10-12, 15-18, 18-21, and 21-25 mm). In order to determine the variation in the chloride concentration as a

function of depth from the exposed surface, the powder was tested for acid soluble chlorides in accordance with Strategic Highway Research Programme 330.

A cylindrical specimen with a length of 100 mm and a diameter of 50 mm is used to calculate the chloride threshold. A simulated pore solution containing 5% NaCl solution was kept submerged in the specimens, which were constructed with an 8mm diameter and 60 mm length TMT rebar implanted in mortar with a water: binder: sand ratio. The specimens were demoulded after 24 hours and water cured (at 25 ± 2 °C) for 28 days. After curing, the specimens are placed in a flash zone environment, where they are submerged in water for 2 days and exposed to the outside air for 5 days. This process is typically repeated in wet and dry cycles. Using saturated calomel electrode (SCE) as the reference and nichrome mesh as the counter electrode, linear polarisation resistance is utilised to measure the polarisation resistance at the conclusion of each cycle. Up to a point when the value drops to 10,000 Ω·cm<sup>2</sup>, the polarisation resistance R<sub>p</sub> was recorded (Ohama et al. 1993). At that point, the cycles were stopped, demonstrating that the initial stages of corrosion had begun. The specimen's chloride concentration is then ascertained by titrating a soluble powder sample extracted by drilling, and the concentration of chloride relative to the proportion of concrete is known as the chloride threshold.

**2.4 Analytical Method**

The average diffusion coefficient is computed using the error function model that is derived from Fick's second law, in compliance with ASTM C1556. This approach assumes a constant diffusion coefficient over time and finds the concrete apparent diffusion coefficient by fitting a numerical model of the chloride ingress to the measured chloride profile.

$$C(x, t) = C_s \left[ 1 - e_{rf} \left( \frac{x}{\sqrt{4D_a t}} \right) \right] \dots\dots\dots (1)$$

where C<sub>s</sub> is the chloride concentration at the surface, C<sub>i</sub> is the initial concentration of the concrete before it is submerged in the exposure solution, and C(x,t) is the chloride concentration at depth x from the surface at time t. Since the initial concentration of chloride in each sample was less than 0.035 mass%, it was presumed that the concentration of chloride in each sample was 0%. The apparent chloride diffusion coefficient (D<sub>a</sub>) is the average value throughout time (t) of exposure (Burriss et al. 2014).

**2.4.1 Service Life Modeling Methodology**

Service life modelling was performed using

Error function model. Diffusivity was predicted for Error function equation using Eq. (2), (3), and (4)

$$D(t) = D_{ref} \left( \frac{t_{ref}}{t} \right)^m \dots\dots\dots(2)$$

$$D_{ref} = 10^{(-12.06+2.4w/cm)} \dots\dots\dots(3)$$

$$m = 0.2 + 0.4 \left( \frac{\% FA}{50} + \frac{\% SG}{70} \right) \dots\dots\dots(4)$$

All analyses were modelled for a concrete column with 40 mm of concrete covering the steel reinforcement in a splash zone. For this work, “service life” corresponds to the years from placement of the concrete until the build-up of chlorides at the level of the steel results in the initiation of corrosion (Athibaranan et al. 2022). An initial estimate of the concrete service life was generated using the software program’s default diffusion and decay coefficient values, based on equations.

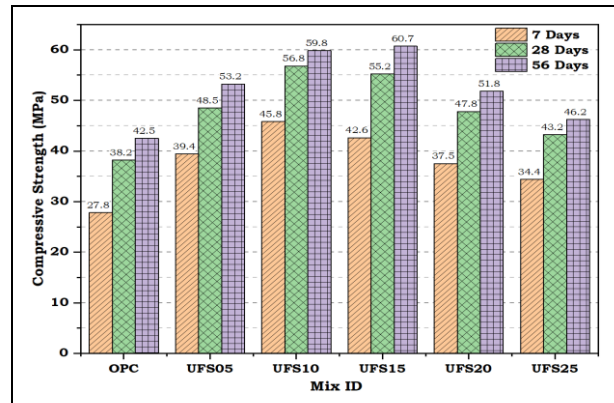


**Fig. 2: Compressive strength of mortar with and without UFS**

**3. RESULTS AND DISCUSSION**

**3.1 Compressive Strength Results**

The mortar specimen with the highest compressive strength is UFS20, which likely corresponds to a 20% UFS replacement of OPC. This suggests that incorporating UFS up to 20% can enhance the compressive strength of the mortar compared to the control group (OPC). There is a possibility that UFS content beyond 20% (UFS25) might lead to a decrease in compressive strength (Fig.2). Overall, the data suggests that UFS replacement can be a beneficial strategy for improving the compressive strength of mortar specimens, likely up to an optimal replacement level. The UFS

particles can fill voids in the cement paste, leading to a denser and stronger microstructure (Athibaranan *et al.* 2022). The UFS can react with the hydration products of OPC to form additional cementitious compounds, further contributing to strength.

The compressive strength was performed to study the mechanical properties of mortar. The results show maximum compressive strength of 60.7 MPa at 56 days strength for the mortar specimen in which cement was replaced by 15% of UFS, showing a 48% increase in strength than control specimen. But in the case of 28-day cube compressive strength, maximum compressive strength is given by 10% UFS replaced specimen which shows an increase in latter age strength percentage of 15% UFS specimen due to its pozzolanic action.

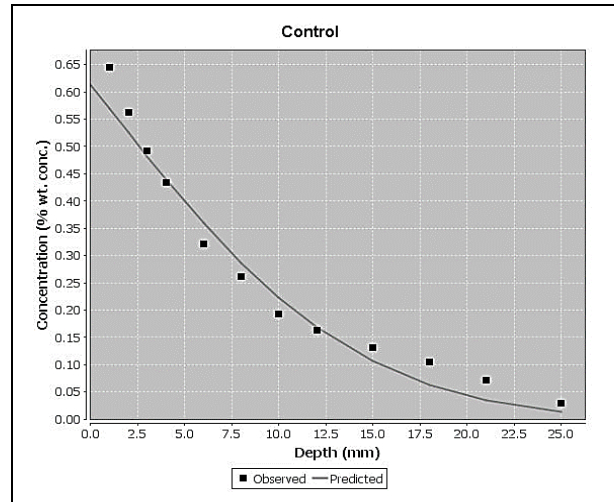
### 3.2 Apparent Chloride Diffusion and Surface Chloride Concentration Results

Table 3 shows the apparent chloride coefficient of UFS replaced specimen values which were found to be much lower than control specimen. Hence, this proves the ability of UFS as micro filler that reduces the permeability of the mortar. The surface chloride concentration and diffusion coefficient are found for all the UFS mixed mortar (0%, 10%, 15%, 20%, 25% UFS replacement) by fitting the curve of error function equation for the plot between depth vs chloride content as shown in Fig. 3 to Fig. 8.

The apparent chloride diffusion coefficient is a key indicator of the transport rate of chlorides within concrete or mortar specimens. In this study, the apparent chloride diffusion coefficients exhibit a complex trend with varying levels of UFS replacement. Notably, the control specimen demonstrates the highest apparent chloride diffusion coefficient at  $25 \times 10^{-12} \text{ m}^2/\text{s}$ , indicating relatively rapid chloride ingress compared to specimens with UFS replacement. The high apparent chloride diffusion coefficient in the control specimen can be attributed to the absence of UFS, which typically enhances the microstructure and pore refinement in cementitious materials. The coarser pore structure in the control specimen provides pathways for accelerated chloride penetration, leading to higher diffusion coefficients.

**Table 3. Values of apparent chloride diffusion coefficient and surface chloride concentration**

W/B	Mixture	$D_{cl}$ , ( $\times 10^{-12} \text{ m}^2/\text{s}$ )	$C_{ss}$ , mass%
0.4	OPC	25	0.613
0.4	UFS05	13.4	0.646
0.4	UFS10	5.35	0.695
0.4	UFS15	9.59	0.553
0.4	UFS20	10.7	0.487
0.4	UFS25	15.5	0.509



**Fig. 3: Depth vs chloride concentration of OPC**

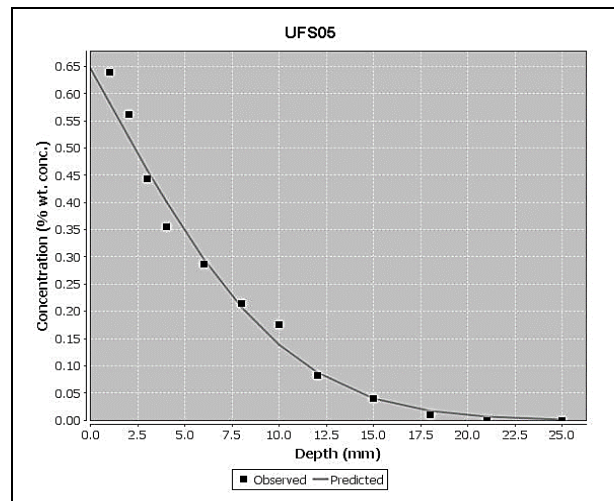


**Fig. 4: Depth vs chloride concentration of UFS05**

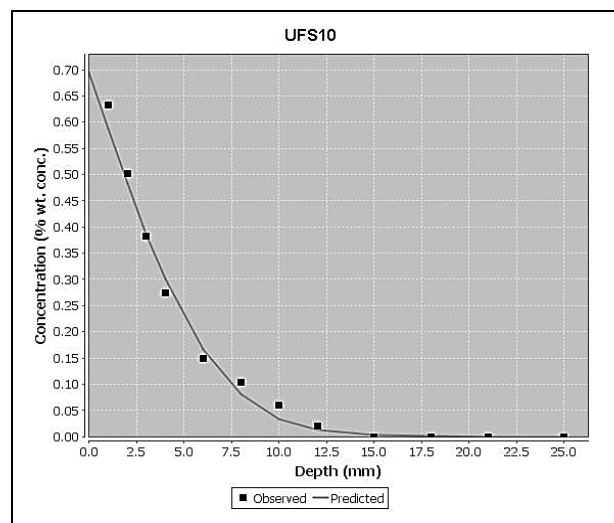


**Fig. 5: Depth vs chloride concentration UFS10**

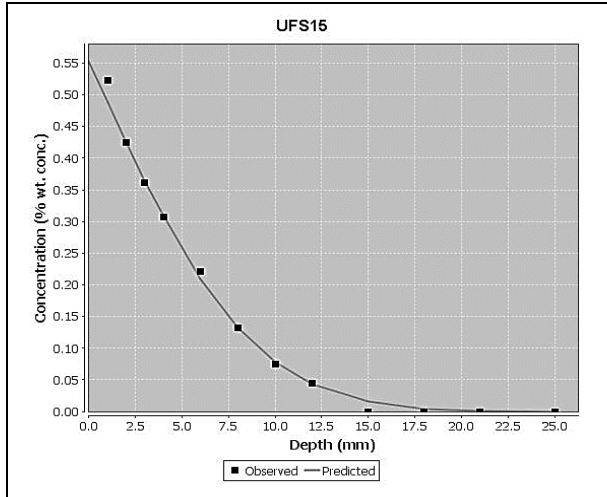


Fig. 6: Depth vs chloride concentration UFS15

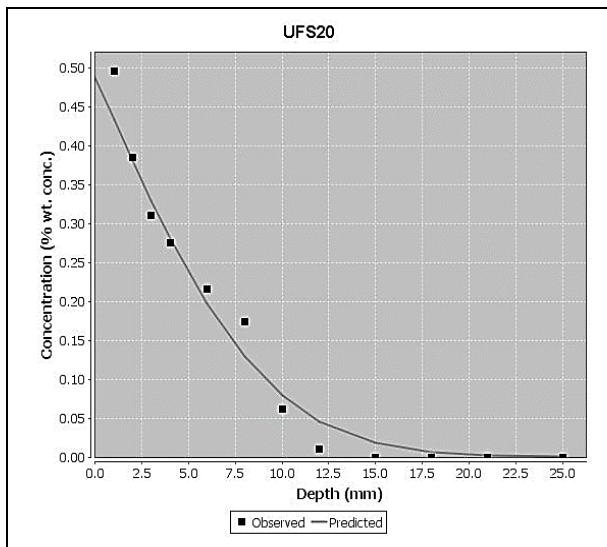


Fig. 7: Depth vs chloride concentration UFS20

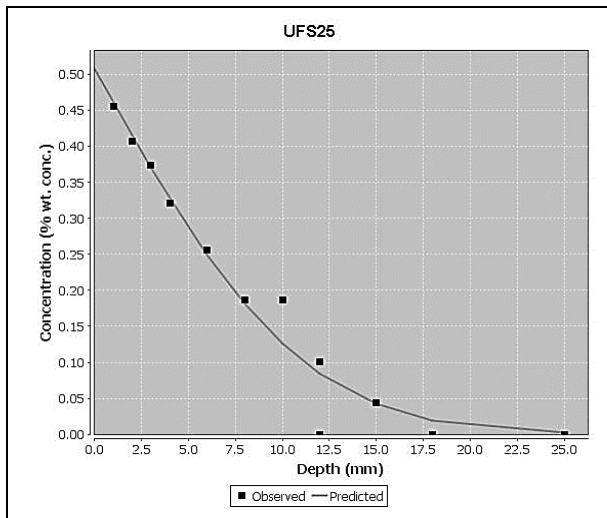


Fig. 8: Depth vs chloride concentration UFS25

As the percentage of UFS replacement increases from 5% to 25%, the apparent chloride diffusion coefficients exhibit varying trends. The 5% replacement shows a notable reduction in diffusion coefficient to  $13.4 \times 10^{-12} \text{ m}^2/\text{s}$ , indicating an initial improvement in chloride resistance. However, further increases in UFS replacement to 10% and 15% result in even lower diffusion coefficients  $5.35 \times 10^{-12} \text{ m}^2/\text{s}$  and  $9.59 \times 10^{-12} \text{ m}^2/\text{s}$ , respectively, suggesting enhanced chloride resistance with higher slag content. Interestingly, beyond 15% replacement, the apparent chloride diffusion coefficients showed an increasing trend again, with values of  $10.7 \times 10^{-12} \text{ m}^2/\text{s}$  for 20% replacement and  $15.5 \times 10^{-12} \text{ m}^2/\text{s}$  for 25% replacement. This phenomenon may indicate diminishing returns or the onset of other factors influencing chloride transport such as, changes in pore connectivity or composition at higher slag content.

### 3.3. Chloride Threshold Results

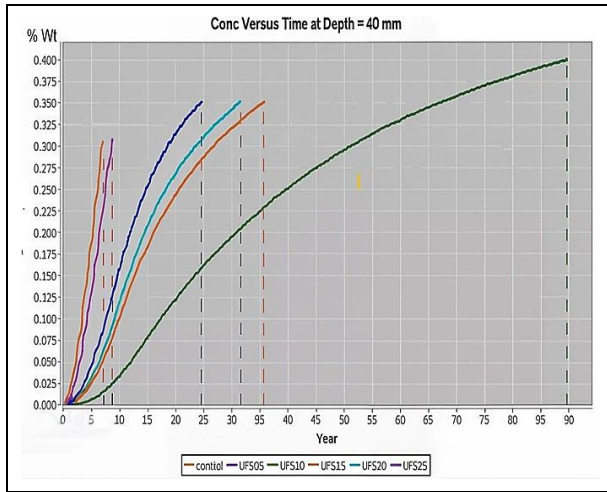
As in Table 4, the chloride threshold for the UFS10 is higher than all other mixes. It shows that the chloride binding capacity of UFS10 is more compared to other mixes.

Table 4. Values of chloride threshold concentration for each mix

W/B	Mixture	Ct, mass%
0.4	Control (OPC)	0.40
0.4	UFS05	0.36
0.4	UFS10	0.36
0.4	UFS15	0.35
0.4	UFS20	0.34
0.4	UFS25	0.30

The chloride threshold, defined as the critical chloride concentration at which corrosion of embedded reinforcement is initiated, is a crucial parameter in assessing the durability and service life of concrete or mortar structures exposed to chloride-rich environments (Dordi *et al.* 2013). The results obtained for the chloride threshold concentrations for control specimens and those incorporating different percentages of UFS replacement (5%, 10%, 15%, 20%, and 25%) provide valuable insights into the influence of slag content on the susceptibility to chloride-induced corrosion. The control specimen exhibits a chloride threshold concentration of 0.32%, indicating the critical chloride level required to initiate corrosion in the absence of UFS. This value serves as a reference point for comparing the performance of specimens with varying slag content. The relatively low chloride threshold highlights the inherent vulnerability of conventional mortar to chloride-induced corrosion and underscores the importance of adopting strategies to enhance durability in chloride-exposed environments.

The chloride threshold concentrations for specimens incorporating UFS replacement show notable variations depending on the slag content. The specimen with 5% UFS replacement demonstrates a chloride threshold concentration of 0.35%, representing a slight increase compared to the control specimen. This enhancement suggests a beneficial effect of incorporating a small percentage of slag in improving the resistance to chloride-induced corrosion, possibly attributed to pore refinement and chloride binding mechanisms associated with slag (Petcherdchoo *et al.* 2013). Similarly, specimens with 10% and 15% UFS replacement exhibit chloride threshold concentrations of 0.4% and 0.35%, respectively. These values indicate further improvements in chloride resistance compared to the control specimen, suggesting that moderate levels of slag replacement contribute to enhanced durability by mitigating the ingress of chlorides and delaying the onset of corrosion. Interestingly, specimens with higher levels of UFS replacement (20% and 25%) display chloride threshold concentrations of 0.35% and 0.30%, respectively. While these values are comparable to or slightly lower than those observed for lower slag replacement levels, they suggest that increasing slag content beyond a certain threshold may not provide additional benefits in terms of chloride resistance or corrosion inhibition.



**Fig. 9: Service life time (Years) vs chloride threshold concentration**

### 3.4. Life-cycle Assessment Results

The service life time predicted by using error function model is shown in Fig.9. The cement replaced by 10% UFS gives excellent service life compared with other specimens. All the UFS replaced specimens were predicted to give longer durability than OPC.

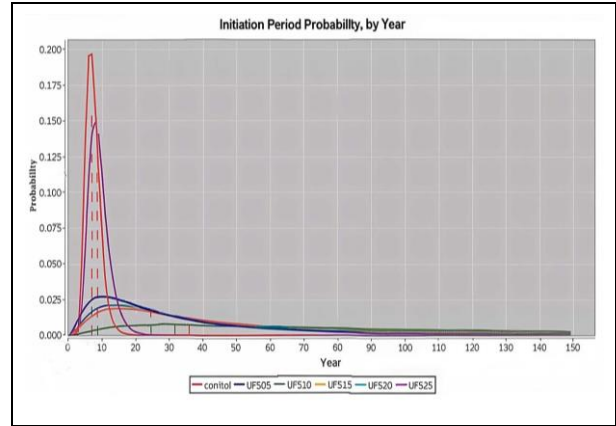


**Fig. 10: Probabilistic corrosion initiation vs Service life years**

The control group, with no UFS replacement, exhibits the highest and fastest increase in corrosion initiation probability. This indicates that UFS replacement offers a protective effect against corrosion. The curves for UFS replaced specimens (5%, 10%, 15%, 20%, and 25%) show a lower probability of corrosion initiation compared to the control group, suggesting that UFS addition improves the corrosion resistance of concrete. While all UFS replacements provide benefit, a definitive trend towards an optimal UFS content for maximum corrosion resistance cannot be established from this graph (Fig. 10). The timeframe for corrosion initiation cannot be directly determined. However, it is evident that higher UFS content delays the onset of corrosion compared to the control group.

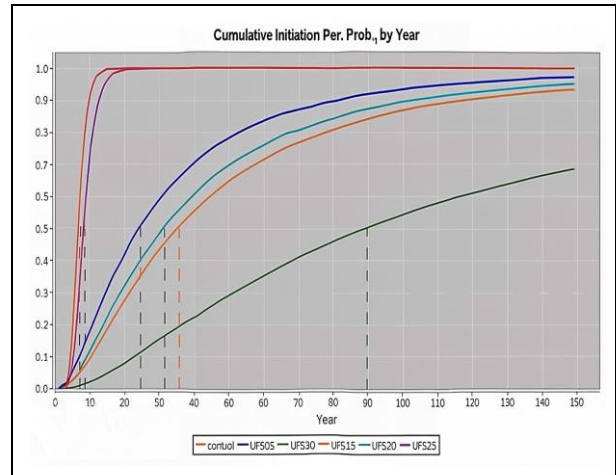


**Fig 11: Cumulative Initiation vs years**

The above results show the probability of corrosion is lesser for the UFS replaced specimens compared to control specimen. The results show the probabilistic service life time of UFS10 is two times more than the control specimen (Fig. 11).

#### 4. CONCLUSION

The compressive strength of UFS10% replaced specimen gives a maximum compressive strength of 56.8 MPa which is 48% higher than that of control specimen, which may be due to formation of more calcium silicate hydrates since more silica is present in UFS than OPC. The apparent coefficient value for UFS10% is also found to be lesser than other mixes which may be due the reduction in permeability of the specimen by the micro fillers present in UFS. The other UFS specimens are also found to have considerable reduction in apparent coefficient value compared to control specimen. Binary blended cement concrete containing UFS decreases apparent diffusion coefficient and increases  $C_s$ , due to an increased concrete pore structure refinement and chloride binding capacity. The probabilistic service life estimated by error function model based on apparent diffusion coefficient, chloride threshold and age coefficient results for worst case scenario (flash zone) predicts UFA10%, a service life of 90 years which is more than two times the life of OPC which is due to its micro filling ability that strengthens the pore structure against permeability. This data provides strong evidence that incorporating UFS into concrete enhances its resistance to corrosion initiation.

#### FUNDING

This research received no specific grant from any funding agency in the public, commercial, or not-for-profit sectors.

#### CONFLICTS OF INTEREST

The authors declare that there is no conflict of interest.

#### COPYRIGHT

This article is an open-access article distributed under the terms and conditions of the Creative Commons Attribution (CC BY) license (<http://creativecommons.org/licenses/by/4.0/>).



#### REFERENCES

Andrade, C., Castellote, M. and D'Andrea, R., Measurement of ageing effect on chloride diffusion coefficients in cementitious matrices, *J. Nucl. Mater.*, 412, 209-216 (2011).  
<https://doi.org/10.1016/j.jnucmat.2010.12.236>

- Andrade, J. J. O., Possan, E. and Dal Molin, D. C. C., Considerations about the service life prediction of reinforced concrete structures inserted in chloride environments, *J. Build. Pathol. Rehabil.*, 2(1), 6-8 (2017).  
<https://doi.org/10.1007/s41024-017-0025-x>
- Angst, U., Elsener, B., Larsen, C. K. and Vennesland, O., Critical chloride content in reinforced concrete - A review, *Cem. Concr. Res.*, 39, 1122-1138 (2009).  
<https://doi.org/10.1016/j.cemconres.2009.08.006>
- Athibaranan, S. and Jayakumar, K., Effect of curing regimes on microstructural and strength characteristics of UHPC with ultra-fine fly ash and ultra-fine slag as a replacement for silica fume, *Arabian J. Geosci.*, 15, 345 (2022).  
<https://doi.org/10.1007/s12517-022-09617-y>
- Athibaranan, S., Karthikeyan, J. and Rawat, S., Investigation on service life prediction models of reinforced concrete structures exposed to chloride laden environment, *J. Build. Pathol. Rehabil.*, 7(16) (2022).  
<https://doi.org/10.1007/s41024-021-00149-8>
- Burris, L. E. and Riding, K. A., Diffusivity of binary and ternary concrete mixture blends, *ACI Mater. J.*, 111(4), 373 (2014).  
<https://doi.org/10.14359/51686826>
- Dordi, C. M., Vyasa Rao, A. N. and Santhanam, M., Microfine ground granulated blast furnace slag for high performance concrete, *Third International Conference on Sustainable Construction Materials and Technologies*, (2013).
- Hooton, R. D. and Rajani, B., Chloride threshold values to initiate corrosion in reinforced concrete, *Cem. Concr. Res.*, 25(2), 287-294 (1995).  
[https://doi.org/10.1016/0008-8846\(94\)00125-6](https://doi.org/10.1016/0008-8846(94)00125-6)
- Jones, S. Z., Davis, J. M., Molloy, J. L., Sieber, J. R. and Bentz, D. P., Modeling and measuring chloride ingress into cracked mortar, *Fourth International Conference on Sustainable Construction Materials and Technologies* (2016).
- Jumaat, M. Z., Mannan, M. A. and Rahman, M. A., Life-cycle cost analysis of repair strategies for reinforced concrete structures, *J. Constr. Eng. Manage.*, 137, 837-848 (2011).  
[https://doi.org/10.1061/\(ASCE\)CO.1943-7862.0000359](https://doi.org/10.1061/(ASCE)CO.1943-7862.0000359)
- Ohama, Y., Birely, N. and Sereda, M., Assessment of chloride threshold in reinforced concrete: Evaluation of methods and factors influencing results, *ACI Mater. J.*, 90(4), 346-356 (1993).
- Park, J. I., Lee, K. M., Kwon, S. O., Bae, S. H., Jung, S. H. and Yoo, S. W., Diffusion decay coefficient for chloride ions of concrete containing mineral admixtures, *Adv. Mater. Sci. Eng.*, 2016, 2042918 (2016).  
<https://doi.org/10.1155/2016/2042918>

- Park, K. B., Lee, H. S. and Wang, X. Y., Prediction of time-dependent chloride diffusion coefficients for slag-blended concrete, *Adv. Mater. Sci. Eng.*, 2017, 1901459 (2017).  
<https://doi.org/10.1155/2017/1901459>
- Petcherdchoo, A., Time dependent models of apparent diffusion coefficient and surface chloride for chloride transport in fly ash concrete, *Constr. Build. Mater.*, 38, 497-507 (2013).  
<https://doi.org/10.1016/j.conbuildmat.2012.08.041>
- Vivek, S., Priya, V., Thanukrishna, K. and Vignesh, R., Experimental investigation on bricks by using cow dung, rice husk, egg shell powder as a partial replacement for fly ash, *Asian Review of Civil Engineering*, 9(2), 1-7 (2020).  
<https://doi.org/10.51983/tarce-2020.9.2.2556>